HEAT AND MASS TRANSFER FROM MOIST AIR FLOWING OVER MOVING WATER FILM I-THEORETICAL STUDY

دراسة انتقال الحرارة والكتلة لتيارمن الهواء الرطب فوق طبقة ماء متحرك I – دراسة نظرية

M.G. Mousa

Mechanical Power Engineering Dept., Faculty of Engineering, Mansoura University, Mansoura, Egypt.
Email :Mgmousa@mans.edu.eg

خلاصة البحث:

فى هذا البحث تم عمل دراسة نظرية لإنتقال الحرارة والكتلة الأنيين لسريان من الهواء على سطح ماء متحرك . لإتمام الدراسة النظرية تم إفتراض أن سريان الهواء فوق سطح الماء رقائقى ومستقر وقد تم وضع المعادلات الحاكمة للسريان فى صورة تفاضليةلا بعدية لحلها عدديا وهذه المعادلات هى معادلة السريان ومعادلة الحركة ومعادلة الطاقة ومعادلة التركيز وذلك باستخدام تعريف مناسب لكل من المتغيرات المستقلة والتابعة وبحل هذه المعادلات عدديا أمكن الحصول على توزيع كل من السرعة ودرجة الحرارة والتركيز اللابعدية. أيضا تم الحصول على رقم نوسلت الموضعى ورقم شيروود الموضعى كدالة فى رقم رينولدز عند مواضع مختلفة .

وللتأكد من صلاحية النموذج النظرى تم اجراء مقارنة بين كل من النتائج النظرية الحالية ونتائج معملية من أبحاث أخرى سابقة وكانت نتيجة هذه المقارنة مرضية .

وقد أظهرت النتائج أن رقم نوسلت ورقم شيروود يزيد مع زيادة رقم رينولدز .

Abstract

Heat and mass transfer between a horizontal moving water film and air flowing over the film is theoretically investigated. In the present theoretical model, the flow of air over the moving water film is assumed to be laminar and steady in Cartesian coordinates. The governing equations are the continuity, momentum, energy and concentration equations. These governing equations are in a dimensionless form. By introducing new proper independent and dependent variables, the governing equations are transformed to a set of dimensionless differential equations. A computer program in FORTRAN language is developed to solve this set of equations to determine the distribution of the dimensionless velocity, temperature and concentration. Also, local values of Nusselt and Sherwood numbers for different values of Reynolds number are calculated.

Comparison between the obtained results and the previous works show good agreement. The results show that, Nusselt and Sherwood numbers increase with increasing Reynolds number.

Keywords: Theoretical study- Moist air - Heat and mass transfer, Evaporation, Laminar flow.

NOMENCLATURE

C	Concentration of water vapor in the flowing air	kg/m^3
C^*	Dimensionless concentration, $C^* = \frac{C - C_\infty}{C_w - C_\infty}$	--
c_p	Specific heat at constant pressure	J/kg K
D	Diffusion coefficient	m^2/s
d_1	Half the vertical height of the duct	m
h	Heat transfer coefficient	$W/(m^2.\ ^\circ C)$
h_m	Mass transfer coefficient	m/s
h_{fg}	Latent heat of vaporization	J/kg
k	Thermal conductivity	W/m K
kr	Relative thermal conductivity, k_2/k_1	--
L	Length of water panel	m
L^*	Dimensionless length, L/d_1	--
Nu	Nusselt number , $Nu = \frac{h\ (2d_1 - y)}{k}$	--

Accepted June 30, 2005.

p	Pressure	Pa
Pe	Peclet number, Pe=Re Pr	--
Pr	Prandtl number, $\mathrm{Pr}=\frac{\mathrm{cp}\mu}{\mathrm{k}}$	--
q_w	Heat flux at the wall	W/m^2
Re	Reynolds number, $\mathrm{Re}=\frac{u_1\ d_1}{\nu}$	--
Sc	Schmidt number, $\mathrm{Sc}=\frac{\upsilon}{D}$	--
Sh	Sherwood number, $\mathrm{Sh}=\frac{h_m\cdot(2d_1-y)}{D}$	--
T	Temperature	K
T_w	Wall temperature	K
T_∞	Ambient temperature	K
u, w	x- and z- components of velocity	m/s
U, W	Dimensionless velocity components in X- and Z-directions	--
x, z	Horizontal and vertical coordinate	m
X, Z	Dimensionless horizontal and vertical coordinate	--
y	height of water in the duct	m

Greek Symbol

α	Thermal diffusivity	m^2/s
β	Velocity ratio, u_{2i}/u_{1i}	---
ψ	Stream function	m^2/s
μ	Dynamic viscosity of fluid	kg/m.s
ν	Kinematics viscosity of fluid	m^2/s
ρ	Density	kg/m^3
θ	Dimensionless temperature; $\theta=\frac{T-T_\infty}{T_o-T_\infty}$	--
Π	Dimensionless group, $\Pi=\frac{D h_{fk}}{k_1(T_o-T_\infty)}(C_o-C_\infty)$,	--

subscript

1 :	Air	o :	interface	*av* :	*average*
2 :	Water	∞ :	free stream	*i* :	*inlet*

1. INTRODUCTION

Heat and mass transfer processes through air-water interfaces are of a major importance in many engineering applications. Analysis of heat and mass transfer from a gas-liquid interface is of particular interest for water thermal pollution where, an air stream flowing parallel to surface of water reservoir, creek, or river is used to dissipate heat. Also mass transfer problems with phase change, like evaporation, involve heat transfer, and the solution needs to be analyzed by considering simultaneous heat and mass transfer. Some examples of simultaneous heat and mass transfer are drying, evaporative cooling, transpiration cooling, combustion of fuel droplets, cooling by dry ice …etc.

Heat and mass transfer govern the process of evaporation from a water surface into airflow. The boundary layer, between air-water flows, incorporates a resistance to both heat and mass transport processes. At

low temperatures the process is mainly heat transfer controlled, since the concentration difference across the boundary layer is large as compared to a rather small temperature difference. At low temperature difference, the required heat for vaporization of water at the surface to the flowing air is transferred by convection from the flowing air stream and by conduction from the water under the surface due to the sensible heat of the water itself. With increasing gas temperature the temperature difference between the surface and gas, and consequently, the heat transfer rate increases. The concentration difference increases as well because of the combined increase in temperature and saturation pressure at interface. Consequently, the whole process of evaporation becomes mass transfer controlled and the mass transfer resistance is the governing factor.

In pure superheated steam the mass transfer resistance does not exist, since the gas consists only of the evaporating species. This explains why the evaporation into pure superheated vapor is greater than into dry air at higher temperatures.

Evaporation of liquid into its own vapor-air mixture is a problem of coupled heat and mass transfer, which was studied by Schwartze and Brocker (2000). The obtained model can be predicted, theoretically, the effect of evaporation rate and the inversion temperature for different drying process. Also, it is useful in the design of drying processes and estimation of the feasibility of different process options.

H. Charles Newton and Masud Behnia (2000) studied the prediction of pressure loss and void fraction in gas – liquid pipe flows. The two-dimensional model is solved in each phase, for low Reynolds number only. The only empirical information required in this approach, was specification of the flow.

Eames et al. (1997) have collected a review on the evaporation coefficient of water. It is concluded that, molecular collision in the vapor phase and heat transfer limitation in the liquid phase can have a considerable influence on experimental evaporation rates.

Combined heat and mass transfer processes that occur when water evaporates from a flowing film in an inclined channel to air stream, have been investigated by Zheng and Worek (1996). It was found that the combined heat and mass transfer in film evaporation can be enhanced by adding rods to the plate surface to agitate mechanically the flowing water film and air stream.

Sheikholeslami and Watkinson. (1992) examined the effect of steam content on the rate of evaporation of water into moist air and superheated steam at elevated temperatures. Their experimental results confirmed the existence of inversion point temperature, above which the rate of evaporation of water increases with increasing in the steam content of the medium.

Kuan-Tzong Lee (1998) examined the mixed convection in horizontal rectangular duct with wall transpiration.

Franca, F. and R. T. Lahey Jr, (1992) was studied use of drift–flux techniques for the analysis of horizontal two phase two component flows

Chow and Chung (1983) investigated, numerically, the evaporation of water for a laminar gas stream over a flat plate using the governing equations for heat and mass transfer, and derived an iterative similarity solution to the problem. Its numerical results show that, for the same mass flux of the free stream, and at low free stream temperatures, water evaporates faster in air than in moist air and in superheated steam. However, the trend is reversed at high free stream temperatures. The combined effects of higher heat transfer coefficients for steam flows and the interfacial temperature depression can explain the existence of the inversion temperature by the presence of air.

In the present work, numerical study of heat and mass transfer from moving a water film to moist air flowing over a water film inside a test section is examined. In most the engineering applications, heat and

mass transfer occur simultaneously and often these are strongly coupled.

2. MATHEMATICAL MODEL

A schematic of physical model under study is shown in Fig.(1), which shows the coordinate system and dimensional nomenclature. The origin of the coordinate system is taken at the point at which the wall under moving liquid The fluids are considered in parallel and co-current motion and the flow is assumed to be laminar, two dimensional, and incompressible. Before contact, the velocity and temperature of both fluids are uniform and correspond to free stream conditions. It is assumed that the fluid properties are constant for the range of temperatures considered. The upper fluid is a mixture of water vapor and air, and the concentration of water vapor in the free stream air is expressed by its mass fraction. The governing equations of this flow consist of the continuity, momentum, energy and concentration equations.

The flow is axi symmetric flow and is assumed to be laminar, and steady. The effect of gravity force and heat dissipation is neglected. Moreover, uniform velocity and temperature profiles, at the inlet of the duct, are assumed.

To put the governing equations in dimensionless form, one can define appropriate dimensionless independent and dependant variables.

Solving the flow describing equations, velocity and temperature distributions throughout flow field can be determined and hence, the physical quantities of the flow can be calculated, such as heat and mass transfer coefficient and Nusselt and Sherwood numbers.

2.1 Governing Equations

In the following analysis, the flow is assumed to be laminar and steady. The used coordinate system is shown in Fig. (1). It is suitable to select the Cartesian coordinate (x,z) to express the flow governing equations. The flow describing equations are continuity, momentum, energy and concentration equations. They can be written as:

$$\frac{\partial u_i}{\partial x}+\frac{\partial w_i}{\partial z}=0 \quad \ldots\ldots\ldots\ldots\ldots\ldots\ldots\ldots\ldots\ldots\ldots\ldots\ldots\ldots \quad (1)$$

$$w_i\frac{\partial u_i}{\partial z}+u_i\frac{\partial u_i}{\partial x}=-\frac{1}{\rho_i}\frac{\partial p_i}{\partial x}+\frac{\mu_i}{\rho_i}\left(\frac{\partial^2 u_i}{\partial x^2}+\frac{\partial^2 u_i}{\partial z^2}\right) \quad \ldots\ldots\ldots\ldots\ldots\ldots\ldots\ldots \quad (2)$$

$$w_i\frac{\partial w_i}{\partial z}+u_i\frac{\partial w_i}{\partial x}=-\frac{1}{\rho_i}\frac{\partial p_i}{\partial z}+\frac{\mu_i}{\rho_i}\left(\frac{\partial^2 w_i}{\partial x^2}+\frac{\partial^2 w_i}{\partial z^2}\right) \quad \ldots\ldots\ldots\ldots\ldots\ldots\ldots\ldots \quad (3)$$

$$w_i\frac{\partial T_i}{\partial z}+u_i\frac{\partial T_i}{\partial x}=\frac{k_i}{\rho_i C_{p_i}}\left(\frac{\partial^2 T_i}{\partial x^2}+\frac{\partial^2 T_i}{\partial z^2}\right) \quad \ldots\ldots\ldots\ldots\ldots\ldots\ldots\ldots\ldots\ldots \quad (4)$$

$$w_1\frac{\partial C_1}{\partial z}+u_1\frac{\partial C_1}{\partial x}=D\left(\frac{\partial^2 C_1}{\partial x^2}+\frac{\partial^2 C_1}{\partial z^2}\right) \quad \ldots\ldots\ldots\ldots\ldots\ldots\ldots\ldots\ldots\ldots \quad (5)$$

Equations (1-5) are the continuity equation, x-momentum equation, z-momentum equations, energy equation and concentration equation respectively. Where w, u are the velocity component in z and x direction. The temperature, concentration, density and specific heat of the fluid at constant pressure are denoted by T, C, ρ and C_p; respectively. In the forgoing equations, μ,

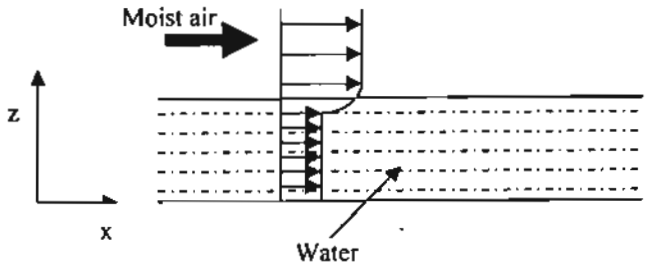

Fig.(1) Schematic diagram of the problem

D and k are dynamic viscosity , diffusion coefficient and thermal conductivity of the fluid; respectively.

Moreover, in the present case, it is satisfactory to solve the governing equations in full domain of the flow field where i equal 1 for moist air, i equal 2 for water.

The flow, heat and mass transfer inside the duct for laminar and steady flow are considered. In this case, the corresponding continuity, momentum, energy and concentration equations (1 – 5) must satisfy the following boundary conditions, as shown in figure (2);

For water:

$$At\ \ x = 0,\ 0 \le z \le y\ :$$
$$w_2 = 0,\ u_2 = u_{2i},\ T = T_{2i}$$
$$At\ \ x = L,\ 0 \le z \le y\ :$$
$$\frac{\partial u_2}{\partial x} = 0,\ w = 0,\ \frac{\partial T_2}{\partial x} = 0$$
$$at\ \ 0 \le x \le L,\ z = 0$$
$$w_2 = 0,\ u_2 = 0,\ T = T_{2w}$$

For moist air:

$$at\ x = 0,\ y < z \le 2d_1\ :$$
$$w_1 = 0,\ u_1 = u_{1i},\ T = T_{1\infty},\ C = C_{1\infty}$$
$$at\ \ 0 < x < L,\ z = 2d_1$$
$$w_1 = 0,\ u_1 = 0,\ T = T_{1\infty},\ C = C_{1\infty}$$

$$at\ x = L,\ y < z \le 2d_1 \qquad (6)$$
$$\frac{\partial u_1}{\partial x} = 0,\ w = 0,\ \frac{\partial T_1}{\partial x} = 0,\ \frac{\partial C_1}{\partial x} = 0$$
$$\text{for interface } at\ \ 0 \le x \le L,\ z = y$$
$$\mu_1 \frac{\partial u_1}{\partial z} = \mu_2 \frac{\partial u_2}{\partial z}$$

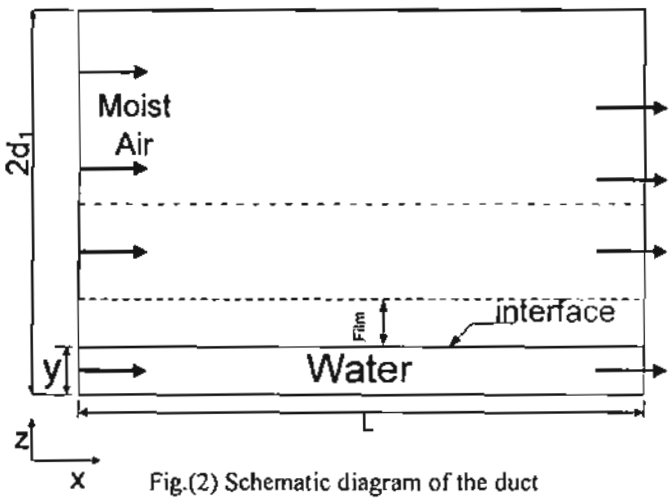

Fig.(2) Schematic diagram of the duct

$$k_1 \frac{\partial T_1}{\partial z} = k_2 \frac{\partial T_2}{\partial z} + D h_{fg} \frac{\partial C}{\partial z}\Big|_{@\ z=y}$$

Where C_o is concentration at interface surface between water and air and u_{1i}, u_{2i}, $T_{1\infty}$ and $C_{1\infty}$ are the inlet velocities, ambient temperature and ambient concentration respectively.

Solving the governing equations (1-5) with their boundary conditions equation (6), one can obtain the velocity and temperature distributions through the flow field. Knowing hydrodynamic and thermal flow field local heat and mass transfer coefficient, and in turn, local Nusselt and Sherwood numbers can be determined. Local heat transfer coefficient is defined according to the following equation:

$$h = \frac{q''}{T_o - T_\infty} = \frac{-k\left(\frac{\partial T_1}{\partial z}\right)_{@\ z=y}}{T_o - T_\infty},$$

$$, h_m = \frac{m'}{C_o - C_\infty} = \frac{-D\left(\frac{\partial C_1}{\partial z}\right)_{@\ z=y}}{C_o - C_\infty} \quad \ldots\ (7\text{-a})$$

And consequently local Nusselt and Sherwood number can be expressed as:

$$Nu = \frac{h \cdot (2d_1 - y)}{k},\ Sh = \frac{h_m \cdot (2d_1 - y)}{D} \quad .(7\text{-b})$$

Average Nusselt and Sherwood numbers can be expressed as:

$$Nu_{av} = \left(\frac{1}{L}\right) \cdot \int_0^L Nu.dx \quad ,$$
$$Sh_{av} = \left(\frac{1}{L}\right) \cdot \int_0^L Sh.dx \quad \ldots\ldots\ (7\text{-c})$$

Equation (7-a) expresses local heat transfer coefficient h as a function of heat flux at plate q'', the lower temperature T_o and the temperature of free stream flow T_∞ and local mass transfer coefficient h_m as a function of mass flux m' , the concentration at water surface and moist air flow. Referring to the definition of local Nusselt number equation (7-b), d_1 is the air flow passage half height and k thermal conductivity, in the definition of local Sherwood number D is diffusion

coefficient. Equations (7-c) represent the definition of average Nusselt and Sherwood numbers.

Seeking for simplicity, one eliminates the pressure term in the momentum equations (2 and 3); by differentiating equation (2) with respect to (z) and differentiating equation (3) with respect to (x) and by subtracting one of the obtained equation from the other equation. Moreover, one introduces flow vorticity ω and stream function ψ where ω and ψ take the following definitions:

$$\omega = \left(\frac{\partial w}{\partial x} - \frac{\partial u}{\partial z}\right), w = -\frac{\partial \psi}{\partial x} \text{ and } u = \frac{\partial \psi}{\partial z} \quad (8)$$

Substitution of the vorticity and stream function definitions, the momentum equation can be rewritten as:

$$\frac{\partial \psi}{\partial z}\frac{\partial \omega}{\partial x} - \frac{\partial \psi}{\partial x}\frac{\partial \omega}{\partial z} = \nu\left\{\frac{\partial^2 \omega}{\partial x^2} + \frac{\partial^2 \omega}{\partial z^2}\right\} \quad \ldots \quad (9)$$

According to the forgoing definitions (8), the vorticity ω can be expressed in term of stream function ψ as:

$$\omega = -\left(\frac{\partial^2 \psi}{\partial x^2} + \frac{\partial^2 \psi}{\partial z^2}\right) \quad \ldots\ldots\ldots\ldots\ldots \quad (10)$$

With the aid of the definitions of stream function and flow vorticity (8), the energy and concentration equations (4,5) can take the following form:

$$\frac{\partial \psi}{\partial z}\frac{\partial T}{\partial x} - \frac{\partial \psi}{\partial x}\frac{\partial T}{\partial z} = \alpha\left\{\frac{\partial^2 T}{\partial x^2} + \frac{\partial^2 T}{\partial z^2}\right\} \quad \ldots(11)$$

$$\frac{\partial \psi}{\partial z}\frac{\partial C}{\partial x} - \frac{\partial \psi}{\partial x}\frac{\partial C}{\partial z} = D\left\{\frac{\partial^2 C}{\partial x^2} + \frac{\partial^2 C}{\partial z^2}\right\} \ldots (12)$$

Where α is the thermal diffusivity and is defined as:

$$\alpha = \frac{k}{\rho Cp}$$

Equations (9-12) must satisfy the following boundary

For water

$x = 0,\ 0 \le z \le y$:

$$\frac{\partial \psi}{\partial z} = -u_{2i},\ \frac{\partial \psi}{\partial x} = 0,\ T = T_{2i}$$

At $x = L,\ 0 \le z \le y$:

$$\frac{\partial^2 \psi}{\partial z^2} = 0,\ \frac{\partial \psi}{\partial x} = 0,\ \frac{\partial T_2}{\partial x} = 0$$

at $0 \le x \le L,\ z = 0$

$$\frac{\partial \psi}{\partial x} = 0,\ \frac{\partial \psi}{\partial z} = 0,\ T = T_{2w}$$

For moist air

at $x = 0,\ y < z \le 2d_1$:

$$\frac{\partial \psi}{\partial x} = 0,\ \frac{\partial \psi}{\partial z} = u_{1i},\ T = T_{1\infty},\ C = C_{1\infty}$$

at $0 < x < L,\ z = 2d_1$

$$\frac{\partial \psi}{\partial x} = 0,\ \frac{\partial \psi}{\partial z} = 0.,\ T = T_{1\infty},\ C = C_{1\infty}$$

at $x = L,\ y < z \le 2d_1$ (13)

$$\frac{\partial \psi}{\partial x} = 0,\ \frac{\partial \psi}{\partial x} = 0,\ \frac{\partial T_1}{\partial x} = 0,\ \frac{\partial C_1}{\partial x} = 0$$

for interface *at* $0 \le x \le L,\ z = y$

$$\mu_1 \frac{\partial^2 \psi}{\partial z^2}\Big|_1 = \mu_2 \frac{\partial^2 \psi}{\partial z^2}\Big|_2$$

$$k_1 \frac{\partial T_1}{\partial z} = k_2 \frac{\partial T_2}{\partial z} + D h_{fg} \frac{\partial C}{\partial z}\Big|_{@z=y}$$

Solving the governing equations (8-12), one can obtain the velocity and temperature distributions through out the flow field. Consequently, the local heat transfer coefficient, and in turn, local Nusselt and Sherwood number

2.2 Dimensionless Form of the Governing Equations

To put the flow describing equations in dimensionless form, one introduces the following definitions of the dependent and independent variables as:

$$\theta = \frac{T - T_\infty}{T_o - T_\infty},\ \Psi = \frac{\psi}{u_{1i} d_1},\ \Omega = \frac{\omega}{u_{1i}/d_1},\ W = \frac{w}{u_{1i}},$$

$$U = \frac{u}{u_{1i}},\ X = \frac{X}{d_1},\ Z = \frac{z}{d_1},\ C^* = \frac{C - C_\infty}{C_o - C_\infty} \quad \ldots(14)$$

Where θ, Ψ, Ω *and* C are the dimensionless temperature, the dimensionless stream function the dimensionless vorticity and dimensionless concentration respectively, W and U are the dimensionless vertical and horizontal velocities respectively. u_f is the reference velocity. The dimensionless Cartesian coordinates and the dimensionless distance are denoted as X *and* Z respectively.

Reynolds, Prandtl, Schmidt and Peclet numbers in the following sections are denoted as Re, *Pr*, Sc and *Pe* respectively, they are defined according to the following relations:

$$Re=\frac{\rho u_{1i} d_1}{\mu}, \quad \Pr=\frac{\nu}{\alpha}, \quad SC=\frac{\nu}{D} \text{ and}$$

$$Pe = Re.Pr \qquad \ldots\ldots\ldots\ldots\ldots (15)$$

Using the above dimensionless forms of the dependent and independent variables (13) and the dimensionless previously mentioned numbers (15), the dimensionless form of the momentum, vorticity, energy and concentration equations can be rewritten as:

$$\frac{\partial\Psi}{\partial Z}\frac{\partial\Omega}{\partial X}-\frac{\partial\Psi}{\partial X}\frac{\partial\Omega}{\partial Z}=\frac{1}{\mathrm{Re}}\left\{\frac{\partial^2\Omega}{\partial X^2}+\frac{\partial^2\Omega}{\partial Z^2}\right\} \quad .(16)$$

$$\Omega=-\left(\frac{\partial^2\Psi}{\partial X^2}+\frac{\partial^2\Psi}{\partial Z^2}\right) \quad \ldots\ldots\ldots\ldots\ldots\ldots (17)$$

$$\frac{\partial\Psi}{\partial Z}\frac{\partial\theta}{\partial X}-\frac{\partial\Psi}{\partial X}\frac{\partial\theta}{\partial Z}=\frac{1}{Pe}\left\{\frac{\partial^2\theta}{\partial X^2}+\frac{\partial^2\theta}{\partial Z^2}\right\} \quad .(18)$$

$$\frac{\partial\Psi}{\partial Z}\frac{\partial C^*}{\partial X}-\frac{\partial\Psi}{\partial X}\frac{\partial C^*}{\partial Z}=\frac{1}{\mathrm{Re}\,Sc}\left\{\frac{\partial^2 C^*}{\partial X^2}+\frac{\partial^2 C^*}{\partial Z^2}\right\} \quad (19)$$

The dimensionless equations (16-19) must satisfy the following boundary conditions in

- For water

$X=0,\ 0\le Z\le y/d_1$:

$$\frac{\partial\Psi}{\partial Z}=-\beta \ , \ \frac{\partial\Psi}{\partial X}=0, \ \theta=0.0 \text{ or } 1.0$$

At $X=L/d_1,\ 0\le Z\le y/d_1$:

$$\frac{\partial^2\Psi}{\partial Z^2}=0 \ , \ \frac{\partial\Psi}{\partial X}=0, \frac{\partial\theta_2}{\partial X}=0$$

at $0\le X\le L/d_1,\ Z=0$

$$\frac{\partial\Psi}{\partial X}=0, \ \frac{\partial\Psi}{\partial Z}=0, \ \theta=0.0 \text{ or } 1.0$$

For moist air

at $X=0,\ y/d_1<Z\le 2$:

$$\frac{\partial\Psi}{\partial X}=0 \ , \ \frac{\partial\Psi}{\partial Z}=-1 \ , \ \theta=0.0 \ , C^*=0.0$$

at $0<X<L/d_1,\ Z=2$

$$\frac{\partial\Psi}{\partial X}=0, \ \frac{\partial\Psi}{\partial Z}=0., \ \theta=0.0 \ C^*=0.0$$

at $X=L/d_1,\ y/d_1<Z\le 2$

$$\frac{\partial\Psi}{\partial X}=0 \ , \ \frac{\partial\Psi}{\partial Z}=0, \frac{\partial\theta_1}{\partial X}=0 \ , \frac{\partial C^*_1}{\partial X}=0$$

for interface *at* $0\le X\le L/d_1,\ Z=y/d_1$

$$\beta\mu_1\frac{\partial^2\Psi}{\partial Z^2}\Big|_1=\mu_2\frac{\partial^2\Psi}{\partial Z^2}\Big|_2$$

$$, \ \theta_1=\theta_2, C_1^*=C_2^*$$

$$\frac{\partial\theta_1}{\partial Z}=kr\frac{\partial\theta_2}{\partial Z}+\prod\frac{\partial C^*}{\partial Z}\Big|_{@Z=y/d_1} \qquad (20)$$

One can solve equations (16-19) with the aid of boundary condition equations to obtain the dimensionless velocity and temperature distributions through out the flow field,. Consequently and with the aid of equation (8), the local Nusselt number can be derived as a function of dimensionless temperature as:

$$Nu=\left(\frac{d\theta}{dZ}\right)_{@Z=y/d_1}, \ Sh=.\left(\frac{dC^*}{dZ}\right)_{@Z=y/d_1} \quad ..(21)$$

2.3 Numerical Technique

Considering a mesh covering the domain of the flow field with lines parallel to the X - axis and Z-axis; and with uniform step size, each node of the mesh is identified by two identifiers i and j, as shown in Fig. (3). Considering the X -direction, the value of X at any column $i+1$, can be evaluated according to the following relations:

$$X_{i+1}=X_i+\Delta X$$

Where i varies from 1 corresponding to X = 0, to M corresponding to X =10, where the total number of columns equal to M. ΔX are the value of step size in X – direction. It is clear that, ΔX depends on the selected total number of columns M and the maximum distance in X- direction. In the same manner, the value of Z at any row j+1 can be evaluated according to the following relation:

$$Z_{j+1}=Z_j+\Delta Z$$

Where j varies from 1 corresponding to Z = 0, to N corresponding to Z = 2 and the step size in Z – direction which depends on the number of rows N and the maximum distance in Z direction.

The partial differential forms of the governing equations are transformed to sets

of linear algebraic equations. Solving these sets of equations, using Gauss-Siedel iterative method, the hydrodynamic, the thermal and concentration flow fields can be

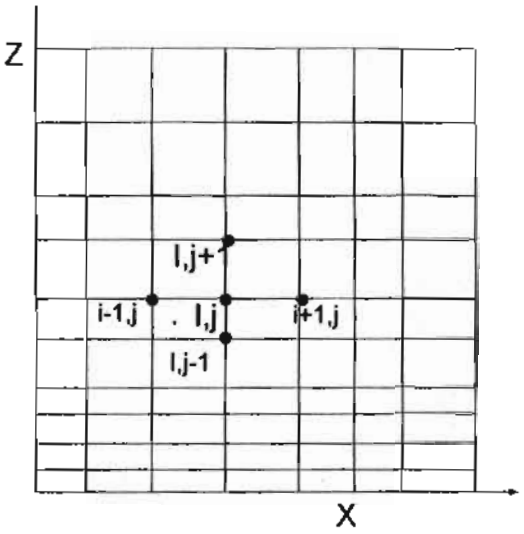

Fig.(3) schematic diagram of the used mesh

obtained. Consequently, local and average Nusselt and Sherwood number can be derived with the aid of their definitions.

2.4 Numerical Procedure

The systems of algebraic equations are solved using Gauss-Siedel iteration method with the above technique. The calculations are carried out on non uniform grid size distribution with factor is 1.001. A non uniform grid with (6000*200) is considered to give grid independent results.

Because finite difference technique is used to solve the momentum and energy equations, the solution can become unstable, i.e., as the solution proceeds; it might diverge increasingly from the actual solution. A simplified analysis of the conditions under which instability occurs is established, the results obtained there indicate that convergence exists if:

$$\Delta X \propto \overline{\Delta Z}^{2}.\mathrm{Re}$$

The solution is carried out row by row. Seeking for rapid convergence of the solution, the obtained values of $(\Omega, \Psi, \theta, C^{*})$ are used in the rest of equations of the rest $(\Omega, \Psi, \theta, C^{*})$'s. This iteration is continued till either the percentage relative error is equal to or less than the prescribed allowable error (maximum error $\leq 1*10^{-7}$).

3. Results and Discussion

In this section the obtained theoretical results are presented and discussed. Accordingly, the theoretical results including,

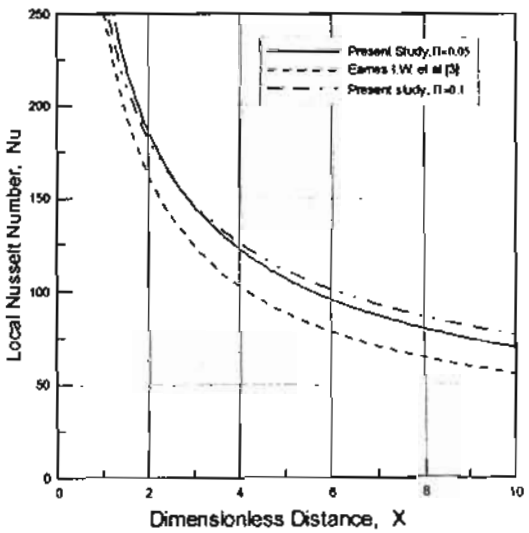

Fig.(4) Comparison between local Nusselt number at Reynolds number equal 2500

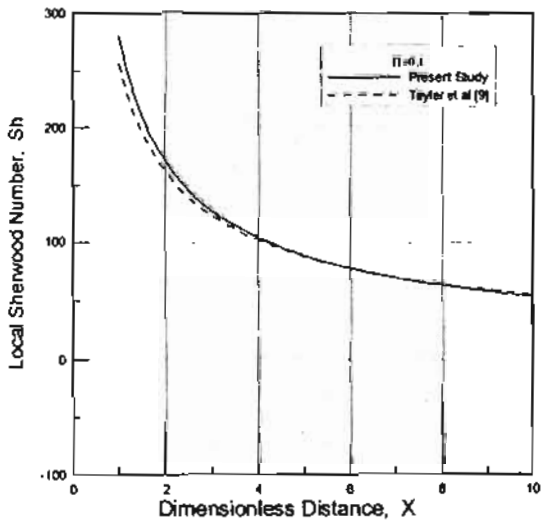

Fig.(5) Comparison between local Sherwood number at Reynolds number equal 3000

derived profiles of dimensionless stream function, dimensionless temperature and concentration in the evaporation film of moist air as well as the local and average heat transfer and mass transfer coefficients are presented. Also a comparison between the present results and that of previous available works are also presented in this section.

In order to check the validity of the model, a comparison is made between the numerical results from present work with the corresponding experimental results reported by Eames, I.W *et al* [2] as shown in Fig. (4).

Also, another check of the model is made by comparing the numerical results from present work with the corresponding experimental results reported by J.Taylor Beard [9] under the conditions of Re = 9000 as shown in Fig. (5)

According to figures (4-5), the present model is fairly valid to predict the flow properties under the studied conditions in all cases of present study.

In this section the effects of the operating parameters such as Reynolds number and velocity ratio are presented. Figures (6-8) show the dimensionless stream function, temperature and concentration distribution at different values of Reynolds number. In general, the stream function, temperature and concentration are taking larger values for larger Reynolds number.

Fig. (6) Illustrates the flow pattern for0020X V VB0020 XZ Zthe flow issues inside a duct at Re = 2500, 5000 and 12000. The streamlines shows that at Re=2500 the flow issues inside the duct and goes parallel to the duct wall rapidly, while at Re=500z ccccccccccccccccccc c 0 appear the stream lines take larger values. At Re=12000 higher values of stream lines inside the duct are obtained.

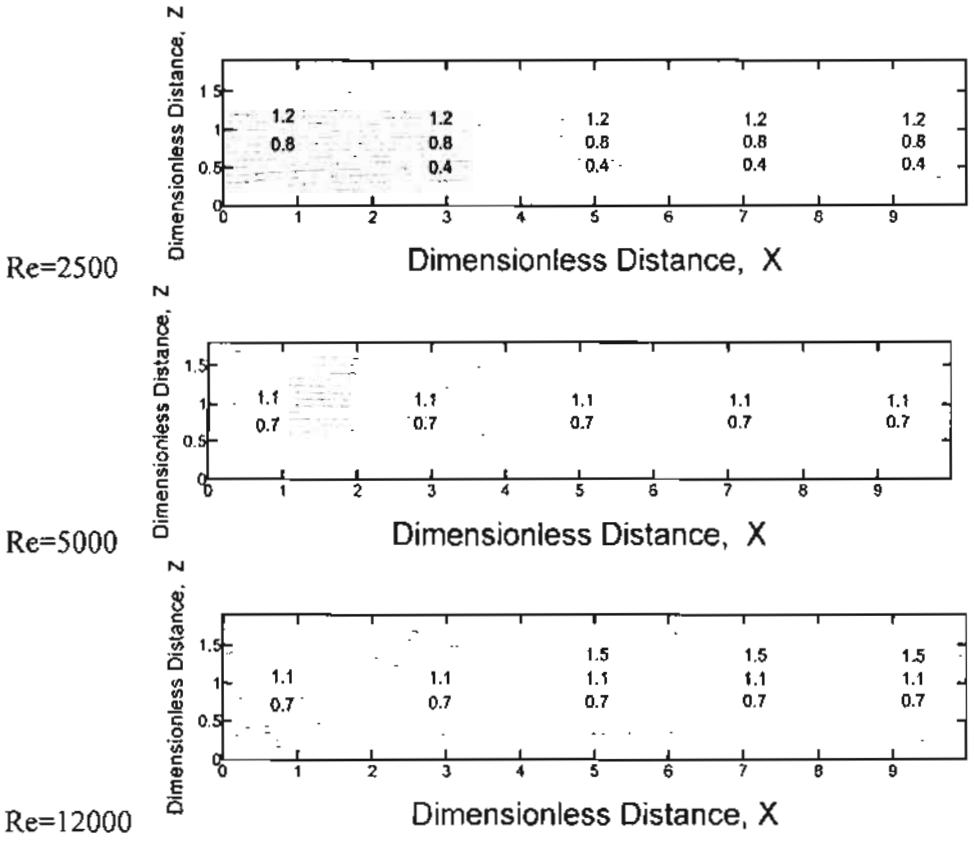

Figure (6) Stream lines for different Reynolds number

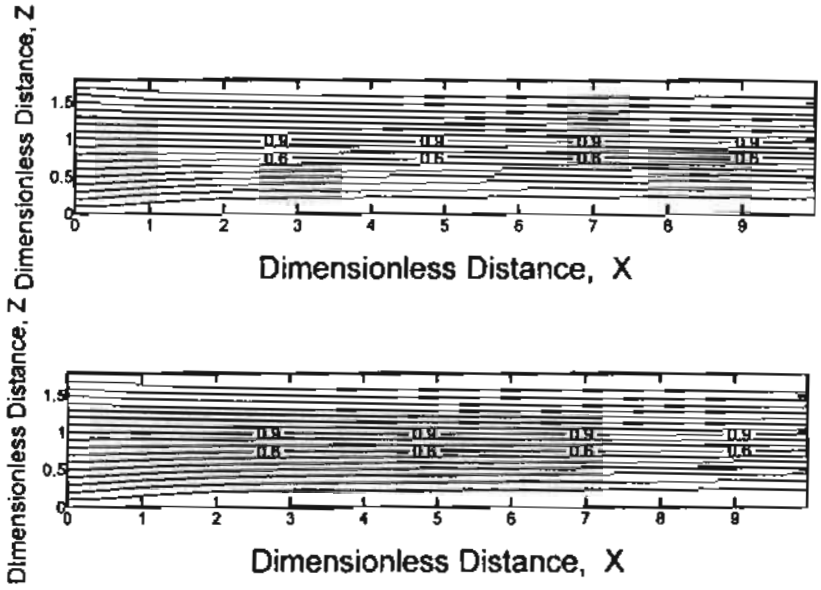

Figure (7) Isotherm lines for different Reynolds number, Π=0.05

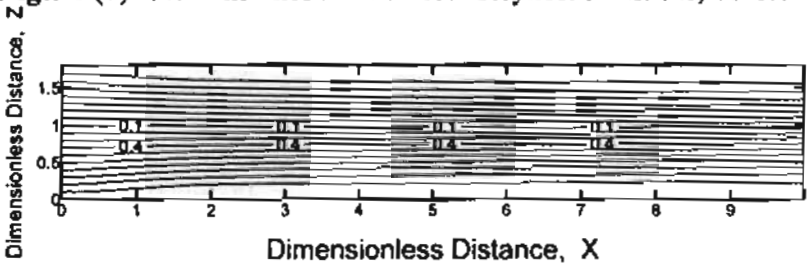

Figure (8) Iso-mass lines for different Reynolds number

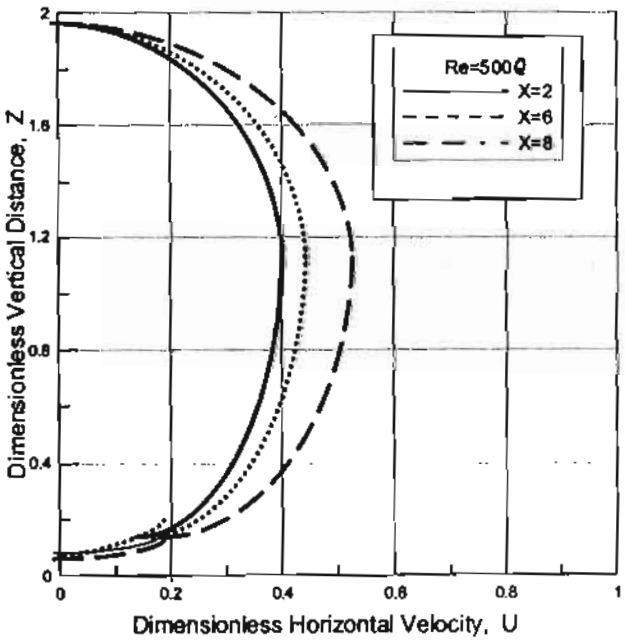

Fig.(9-a) Dimensionless horizontal velocity at Reynolds number equal 5000

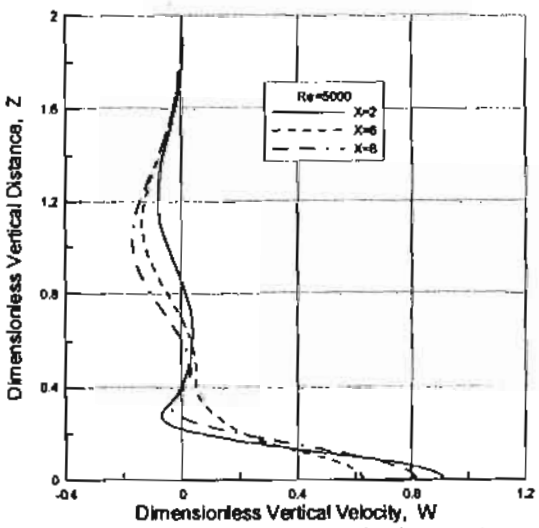

Fig.(9-b) Dimensionless vertical velocity at Reynolds number equal 5000

Fig. (7) Illustrates the isothermal contours for the flow issues inside a duct at

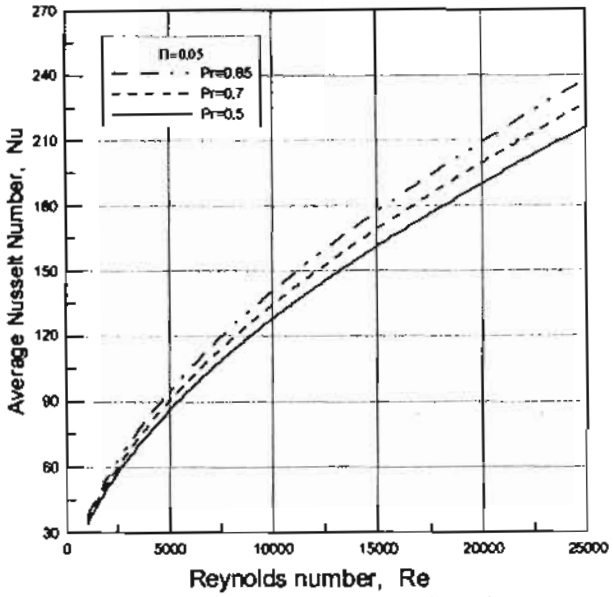

Fig.(10) Variation of the average Nusselt number with Reynolds number

Re = 2500 and 5000. The temperature distribution denotes that the flow temperature is high at the upper wall and get cold far from the upper wall as expected.

Fig. (8) Illustrates the isomass contours for the flow issues inside a duct at Re = 5000. The concentration distribution denotes that the flow concentration is high at the lower wall and get poor far from the lower wall as expected.

Figures (9-a and 9-b) illustrate the velocity distributions in the X- and Z-directions for the flow issues inside the duct at Re = 5000. The figures denotes that, U(Z), the flow velocity takes the full developed shape far from the inlet.

Fig.(10) illustrates the relation between average Nusselt number and Reynolds number for different values of. Prandtl number. The values of Nusselt number number, generally, increase with increasing Reynolds number. The values of Nusselt number number, generally, increase with increasing Prandtl number.

Fig.(11) illustrates the average Sherwood number against Reynolds number for different values of. Schmidt number.

The behavior of Sherwood number looks like that of Nusselt number.

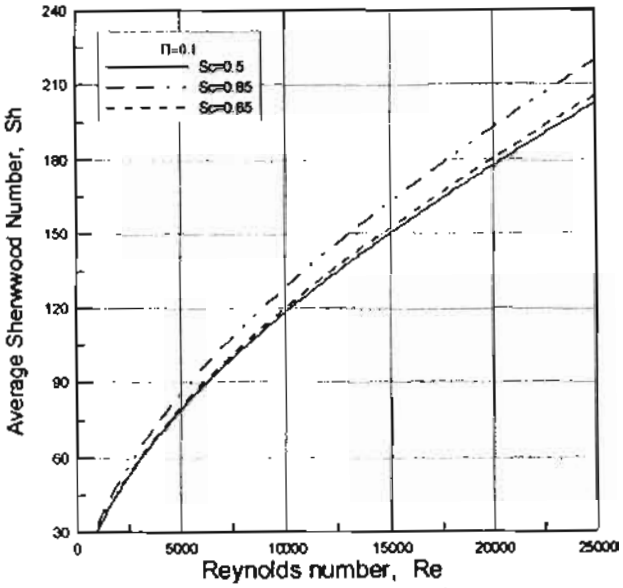

Fig.(11) Relation between average Sherwood number for different values of Reynolds number

Evaporation, and in turn, rate of heat transfer is decreased. But interaction between heat transfer and mass transfer appears in the dimensionless group Π.

Conclusion

In the present study, the evaporation process of water vapor to moist air is, theoretically analyzed. The effects of process parameters are investigated. These parameters are presented by the following dimensionless physical quantities Prandtl, Schmidt, dimensionless group Π and Reynolds numbers. Considering the theoretical proposed model, it is found that the increase of Prandtl and Schmidt numbers cause increase of Nusselt and Sherwood numbers.

The following relations correlate the theoretical results, where the Nusselt and Sherwood numbers are expressed as functions of Reynolds, Prandtl and Schmidt numbers:

$$Nu = 1.145\, Re^{0.44} Pr^{0.34} (1+\Pi^{0.45}),$$
$$Sh = 1.252\, Re^{0.412} Sc^{0.34}$$

The Carried out comparisons between the present work and previous study is exhibit a fairly good agreement.

Comparison between the obtained results and the previous works in case of steady flow shows good agreement. Empirical correlation for Nusselt number and Sherwood number are obtained.

REFERENCES

[1] **Schwartze, J. P. and Brocker, S.**, 2000 "The evaporation of water into air of different humidities and the inversion temperature phenomenon" Int. J. Heat and Mass Transfer Vol. 43, No. 6, pp. 1791-1800.

[2] **H. Charles Newton and Masud Behnia,** 2000 "Brief communication numerical calculation of stratified gas – liquid pipe flows" Int. J. Multiphase flow, Vol. 26, No. 1, PP.327-337

[3] **Eames, I. W., Marr, N. J. and Sabir, H.**, 1997 "The evaporation coefficient of water : a review," Int. J. Heat and Mass Transfer Vol. 40, No. 12, pp. 2963-2973.

[4] **Zheng, G. S. Worek, W. M.**, 1996 "Method of heat and mass transfer enhancement in film evaporation" Int. J. Heat and Mass Transfer Vol. 39, No. 1, pp. 97-108.

[5] **Sheikholeslami, R. and Watkinson, A. P.**, 1992 "Rate of evaporation of water into superheated steam and humidified air" Int. J. Heat and Mass Transfer Vol. 35, No.7, pp. 1743-1751.

[6] **Chow, L. C. and Chung, J. N.**, 1983 "Evaporation of water into a laminar stream of air and superheated steam" Int. J. Heat and Mass Transfer Vol. 26, No.3, pp. 373-380.

[8] **Kuan-Tzong Lee,** 1998 " Mixed convection heat transfer in torizontal rectangular ducts with wall transpiration effects" Int. J. Heat Mass Transfer, Vol. 41,No. 2, pp. 411- 423.

[9] **J.Taylor Beard and C.S. Chen,** 1971 "Convective heat and mass transfer from water surface" water resources research center Virginia Polytechnic Institute and State University Blacksburg, Virginia

[10] **F. Franca and R. T. Lahey Jr,** 1992 "The use of drift–flux techniques for the analysis of horizontal two – phase flows" Int. J. Multiphase flow, Vol. 18, No. 6, PP.787-801